JOURNAL OF MATERIALS SCIENCE 29 (1994) 830–834

Effect of nickel on microwave dielectric properties of $Ba(Mg_{1/3}Ta_{2/3})O_3$

E. S. KIM*, K. H. YOON
Department of Ceramic Engineering, Yonsei University, Seoul, Korea

The dielectric and physical properties of the complex perovskite $Ba(Mg_{1/3}Ta_{2/3})O_3$ system in which magnesium was substituted for nickel from 0.03–0.67 mol%, were investigated in the temperature range 20–110 °C, and the frequency range 10.5–14.5 GHz. As the nickel content was increased, the dielectric constant, the degree of ordering, and the unloaded Q decreased. The temperature dependence of the dielectric constant and the temperature coefficient of resonant frequency of the specimens annealed at 1500 °C for 20 h were found to be greater than those of the specimens sintered at 1650 °C for 2 h. These results are due to the increase in the density, the increase in grain size, and the lattice distortion.

1. Introduction

Recently, complex perovskite compounds with high dielectric constant and low dielectric loss have been found to be good microwave dielectric materials. A number of complex perovskite materials [1–3] and their solid solutions [4–6] have been investigated to develop their microwave dielectric properties and improve their suitability for microwave integrated circuits.

The microwave dielectric properties of complex perovskite compounds are sensitive to crystal structure, such as B-site ordering, and to the microstructure of the specimens. We investigated the effect of ordering and lattice distortion of B-site ions on the microwave dielectric properties of $Ba(Mg_{1/3}Ta_{2/3})O_3$ and confirmed that the loss quality strongly depended on the ordering of B-site ions and on the microstructure [7]. Galasso and Pyle [8] reported that the ordering of B-site ions in the complex perovskite compound $A(B_{0.33}Ta_{0.67})O_3$, was a function of ionic size and charge difference. Desu and O'Bryan [3] explained that the improvement of the loss quality in $Ba(Zn_{1/3}Ta_{2/3})O_3$ ceramics was due to zinc loss and lattice distortion, even after the ordering of B-site ions was completed.

This study describes the effects of small ionic size in the $Ba(Mg_{1/3}Ta_{2/3})O_3$ system, by means of substituting nickel for magnesium ions, on the ordering and lattice distortion of B-site ions, and the effects of ordering and lattice distortion on its microwave dielectric properties.

2. Experimental procedure

The starting materials were high-purity (99.9%) $BaCO_3$, MgO, Ta_2O_5 and $Ni(NO_3)_2 4H_2O$ powders. These powders were weighed and ball-milled together for 24 h with ethanol and zirconia balls. The mixture was then dried and calcined at 1200 °C for 10 h in air. The calcined powders were reground into fine powders and screened through 80 mesh. The screened powder was isostatically pressed into discs under a pressure of 1500 kg cm^{-2} and then sintered at 1650 °C for 2 h in air. The sintered specimens were also annealed at 1500 °C for 20 h in air, the optimum annealing conditions found in our previous work [7]. The structures of sintered specimens and annealed specimens were investigated by X-ray powder diffraction analysis. A least mean square method of analysis was used to calculate lattice parameters [9]. The density of the specimens was measured by an immersion technique. The microstructure of the specimens was observed by SEM (Jeol, JSM820, Japan) and energy dispersive spectroscopy (EDS, Link, AN-10000, UK). Hakki and Coleman's dielectric resonator method [10] in the $TE_{0\,1\,1}$ mode was used to measure the microwave dielectric properties of sintered and annealed specimens. The dielectric constant and unloaded Q were measured over the frequency range 10.5–14.5 GHz. The temperature coefficient of resonant frequency was measured at 10.5 GHz in the range 20–110 °C.

3. Results and discussion

It is reported that $Ba(Mg_{1/3}Ta_{2/3})O_3$ has a hexagonal perovskite structure with magnesium and tantalum showing 1:2 order [8]. The lattice parameter ratio, c/a, has a value greater than $\sqrt{3/2}$ (= 1.2247) resulting from the ordering of B-site ions. Fig. 1 shows the dependence of the lattice parameter ratio, c/a, on the amount of nickel present. The annealed specimens showed a larger lattice parameter ratio than that of the sintered specimens because the ordering of the B-site ions was increased by the annealing process. For both sintered specimens and annealed specimens, the

* *Present address*: Department of Materials Engineering, Kyonggi University, Suwon, Korea.

0022–2461

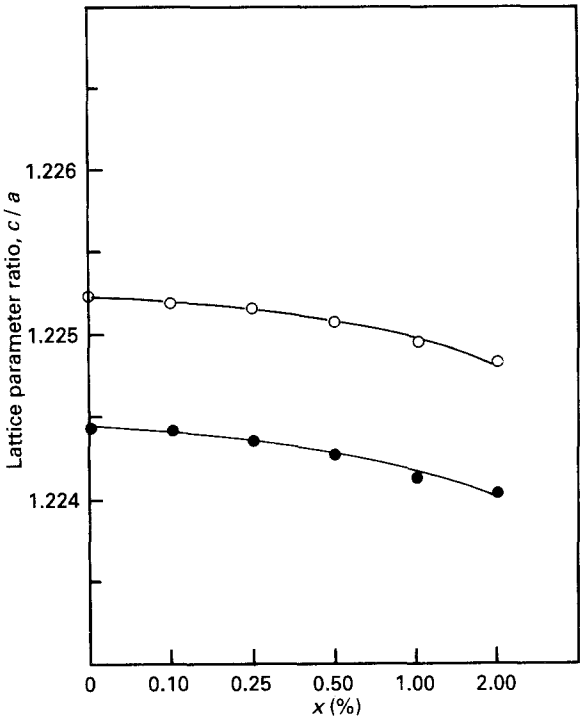

Figure 1 Dependence of lattice parameter ratio, c/a, on the nickel content of $Ba(Mg_{(1-x)/3}Ni_{x/3}Ta_{2/3})O_3$, sintered at (●) 1650 °C for 2 h, and (○) 1500 °C for 20 h.

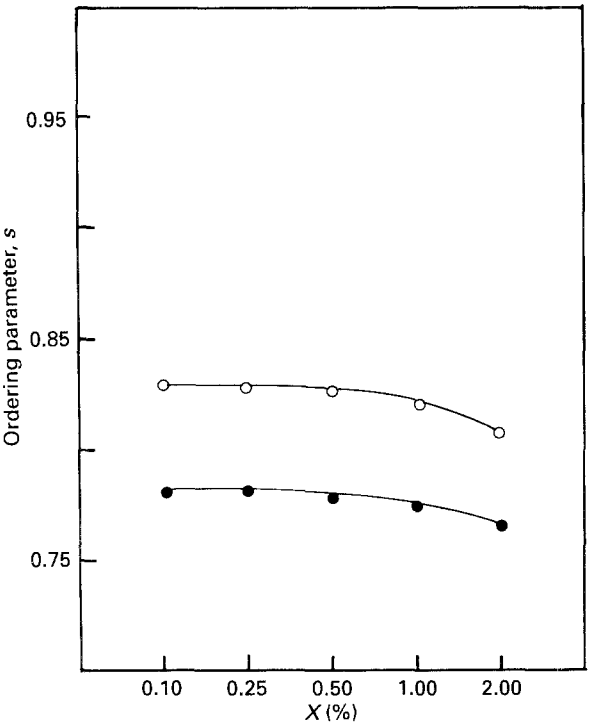

Figure 3 Dependence of the ordering parameter on the nickel content of $Ba(Mg_{(1-x)/3}Ni_{x/3}Ta_{2/3})O_3$, sintered at (●) 1650 °C for 2 h and (○) 1500 °C for 20 h.

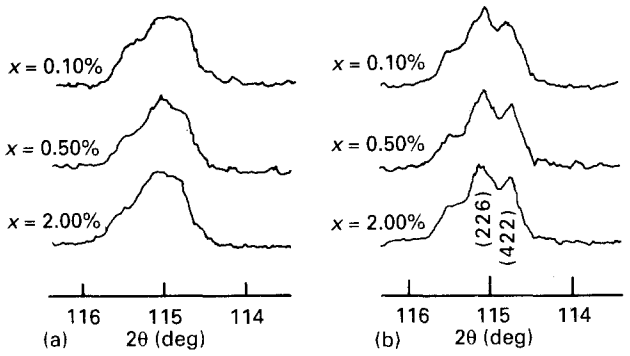

Figure 2 Profiles of (2 2 6) and (4 2 2) reflections of $Ba(Mg_{(1-x)/3}Ni_{x/3}Ta_{2/3})O_3$.

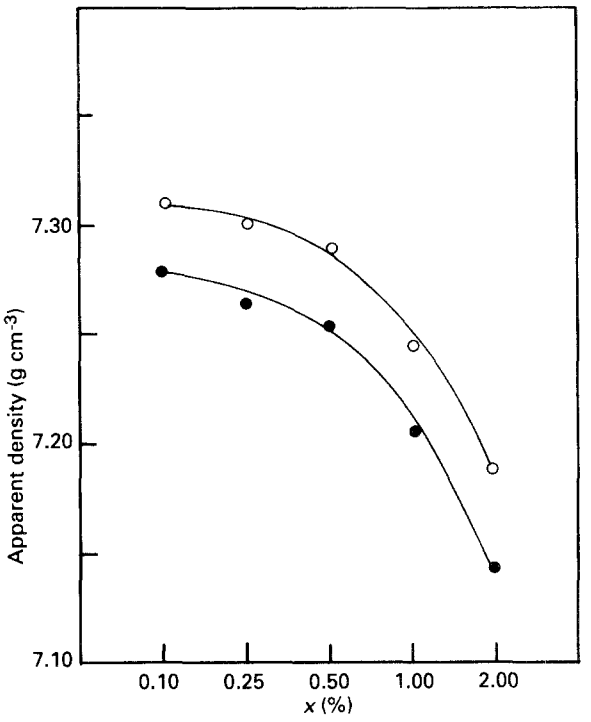

Figure 4 Apparent density as a function of the amount of nickel content for $Ba(Mg_{(1-x)/3}Ni_{x/3}Ta_{2/3})O_3$, sintered at (●) 1650 °C for 2 h, and (○) 1500 °C for 20 h.

lattice parameter ratio was slightly decreased with increasing nickel content. These results are in agreement with our previous work [7].

The lattice distortion due to B-site ordering produces the split of the (4 2 2) and (2 2 6) reflections in X-ray diffraction (XRD) patterns. The profile change of (4 2 2) and (2 2 6) reflections for both sintered and annealed $Ba(Mg_{(1-x)/3}Ni_{x/3}Ta_{2/3})O_3$ specimens is shown in Fig. 2. There was no lattice distortion for the specimens sintered at 1650 °C for 2 h, while that of the annealed specimens could be observed through the entire composition range. This result indicates that the ordering of B-site ions due to thermal energy has a greater effect than the radius mismatch of B-site ions. Fig. 3 shows the ordering parameters of sintered and annealed specimens, which can be quantitatively evaluated from the degree of ordering. As the nickel content increased, the ordering parameters were slightly decreased for both sintered specimens and annealed specimens. For the same composition, the ordering parameters of the annealed specimens were higher than those of the sintered specimens. These results are in agreement with the report [3, 5] that the ordering of B-site ions increased with increasing annealing time.

The apparent density of sintered specimens and annealed specimens is shown in Fig. 4. The density of both sintered and annealed specimens decreased drastically with increasing nickel content. The density of

annealed specimens was higher than that of the sintered specimens with the same composition because the grain size increased through the annealing process, as shown in Fig. 5. The microstructure of both sintered and annealed specimens showed needle-shaped grains appearing in grain boundaries. The number of needle-shaped grains increased with increasing nickel content, and also increased in the annealing process.

Fig. 6 shows the EDS spectra taken from the grains (Fig. 5f, A), and the needle shaped grains in grain boundaries (Fig. 5f, B) of the annealed specimens for a nickel content of 0.67 mol %. It can be seen that the needle-shaped grains in the grain boundaries are depleted for higher barium, magnesium and nickel concentrations and enhanced for high tantalum concentration. It was found that the liquid-phase formation occurred at temperatures of 1500, 1600, 1750, 1100, 2000 and 1780 °C, for the BaO–MgO [11], MgO–Ta_2O_5 [12], Ta_2O_5–$MgTa_2O_6$ [13], BaO–NiO [14], MgO–NiO [15] and Ta_2O_5–NiO [16] systems, respectively. The needle-shaped grains of sintered specimens were due to the BaO and NiO loss of the liquid-phase in the BaO–NiO system, while those of annealed specimens were due to the BaO, MgO and NiO loss of the liquid phase in the BaO–MgO and BaO–NiO systems. Thus, the annealed specimens with the same composition showed more needle-shaped grains than the sintered specimens.

Fig. 7 shows the unloaded Q and dielectric constant measured at 10.5 GHz and 20 °C. Dielectric constants were slightly decreased with the increase in nickel content for both sintered and annealed specimens. This is due to the decrease of density and grain size, as shown in Figs 4 and 5. The annealed specimens with the same composition had a higher dielectric constant than that of the sintered specimens because the annealed specimens had a higher density and larger grain growth than those of the sintered specimens [7, 17].

As the nickel content was increased, the unloaded Q was drastically decreased, resulting from the decrease of density and increase of needle-shaped grains in grain boundaries. These results are in agreement with the reports of Takata and Kageyama [17] and

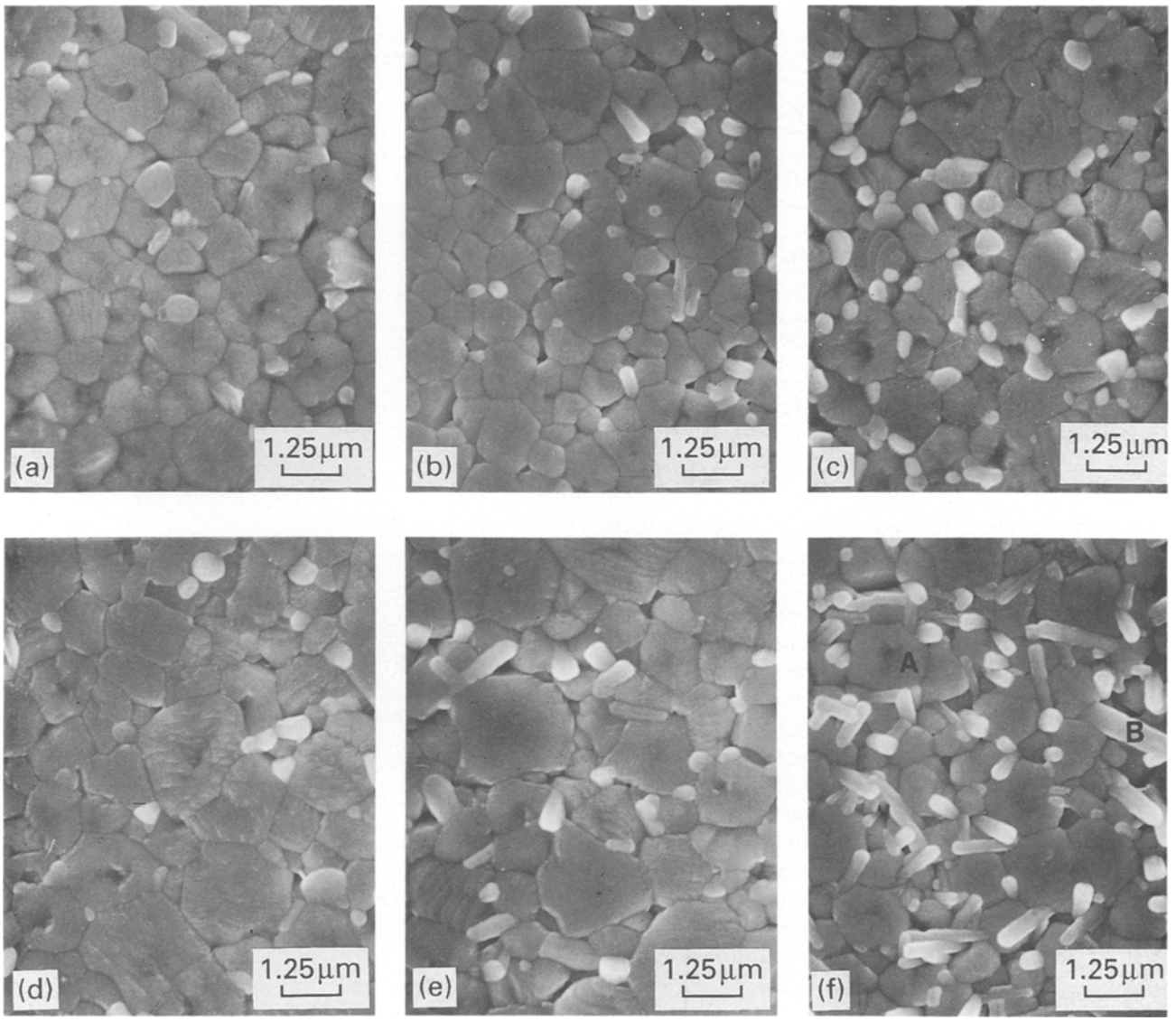

Figure 5 Scanning electron micrographs of $Ba(Mg_{(1-x)/3}Ni_{x/3}Ta_{2/3})O_3$, (a–c) sintered at 1650 °C for 2 h, and (d–f) sintered at 1500 °C for 20 h. (a, c) $x = 0.25\%$, (b, d) $x = 0.5\%$, (c, f) $x = 2.00\%$.

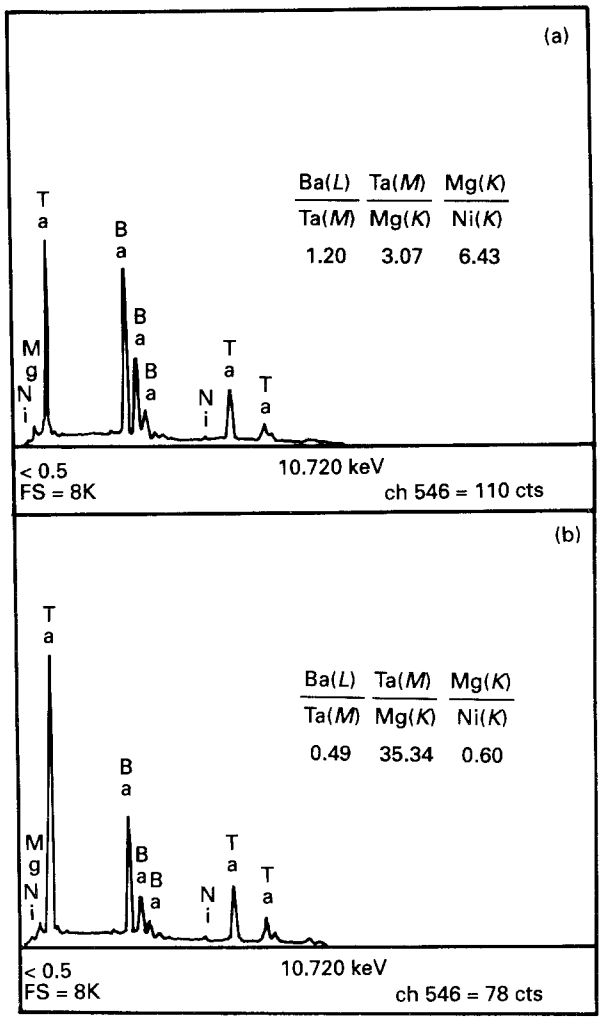

Figure 6 EDS spectra of $Ba(Mg_{0.98/3}Ni_{0.02/3}Ta_{2/3})O_3$ annealed at 1500 °C for 20 h.

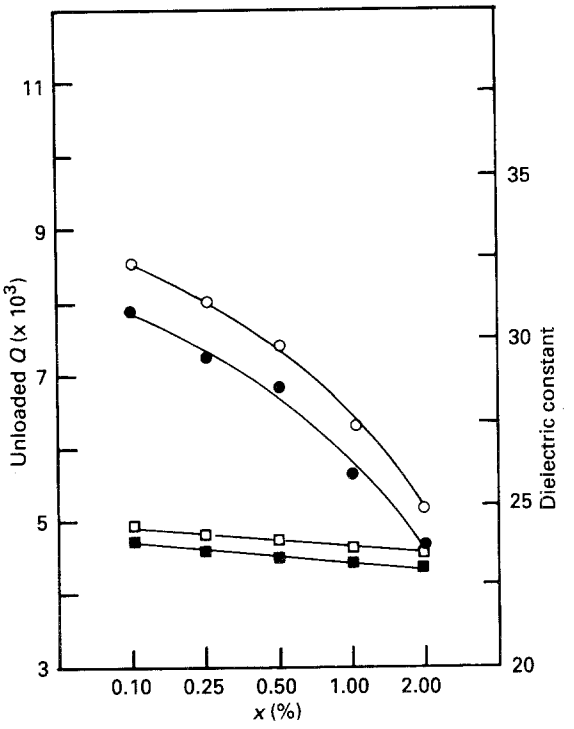

Figure 7 Dependence of (○, ●) unloaded Q and (□, ■) dielectric constant on the nickel content of $Ba(Mg_{(1-x)/3}Ni_{x/3}Ta_{2/3})O_3$, sintered at (■, ●) 1650 °C for 2 h, and (□, ○) 1500 °C for 20 h.

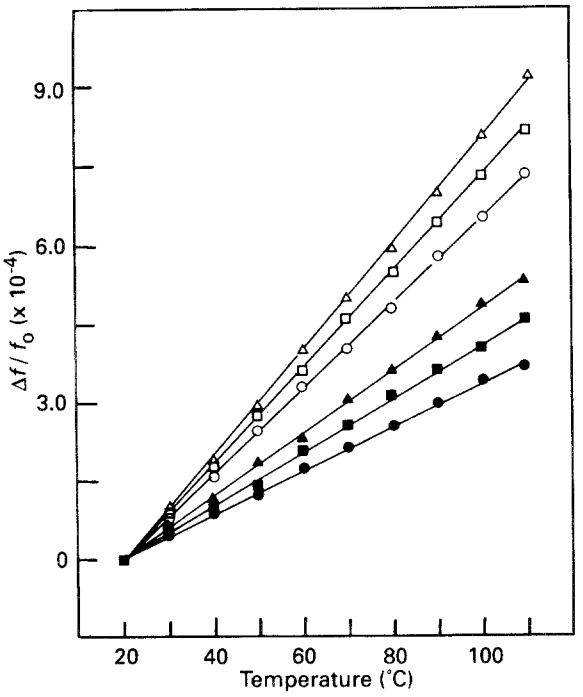

Figure 8 Temperature dependence of resonant frequency for $Ba(Mg_{(1-x)/3}Ni_{x/3}Ta_{2/3})O_3$, sintered at (●, ■, ▲) 1650 °C for 2 h and (○, □, △) 1500 °C for 20 h. (○, ●) $x = 0.10\%$, (□, ■) $x = 0.50\%$, (△, ▲) $x = 2.00\%$.

Wakino *et al.* [18]. The annealed specimens had a slightly higher unloaded Q than that of the sintered specimens with the same composition. The reason is that the annealed specimen has a higher degree of ordering than the sintered specimen, although it forms more needle-shaped grains, magnesium, tantalum-rich phase in the entire composition range.

Fig. 8 shows the temperature dependence of the resonant frequency at 10.5 GHz as a function of temperature in the range 20–110 °C. The temperature coefficient of resonant frequency of the specimen sintered at 1650 °C for 2 h was only slightly changed, while that of the specimen annealed at 1500 °C for 20 h increased greatly with increasing nickel content. These results are due to the lattice distortion and the increase of the temperature coefficient of dielectric constant through the annealing process [7].

4. Conclusions

1. As the nickel content was increased, the dielectric constant and the unloaded Q decreased due to the decrease in density, the decrease in grain size and the decrease in ordering parameters.

2. The needle-shaped grains of the magnesium, tantalum-rich phase were observed in both sintered and annealed specimens. Compared to the sintered specimens, the annealed specimens had a higher dielectric constant, a higher unloaded Q, and a greater temperature dependence of resonant frequency.

Acknowledgement

This work is a part of the G-7 project supported by the KIST.

References

1. S. KAWASHIMA, M. NISIDA, I. UEDA and H. OUCHI, *J. Am. Ceram. Soc.* **66** (1983) 421.
2. S. NOMURA and K. KANETA, *Jpn J. Appl. Phys.* **23** (1984) 507.
3. S. B. DESU and H. M. O'BRYAN, *J. Am. Ceram. Soc.* **68** (1985) 546.
4. M. ONODA, J. KUWATA, K. KANEDA, K. TOYAMA and S. NOMURA, *Jpn J. Appl. Phys.* **21** (1982) 1707.
5. K. ENDO, K. FUJIMOTO and K. MURAKAWA, *J. Am. Ceram. Soc.* **70** (1987) C215.
6. K. H. YOON, B. J. JUNG and E. S. KIM, *J. Mater. Sci. Lett.* **8** (1989) 819.
7. E. S. KIM and K. H. YOON, *Ferroelectrics* **133** (1992) 187.
8. F. GALASSO and J. PYLE, *Inorg. Chem.* **2** (1963) 482.
9. M. U. COHEN, *Rev. Sci. Instrum.* **6** (1963) 68.
10. B. W. HAKKI and COLEMAN, *IRE Trans. Microwave Theory Technol.* **8** (1960) 402.
11. H. VON WARTENBERG and E. PROPHET, in "Phase Diagrams for Ceramists", edited by E. M. Levin, C. R. Robbins, H. F. McMurdie and M. K. Reser (The American Ceramic Society, Columbus, OH, USA, 1964) Fig. 274, p. 113.
12. B. W. KING, J. SCHULTZ, E. A. DURBIN and U. S. DUCKWORTH, *ibid.*, Fig. 273, p. 113.
13. R. S. ROTH, J. L. WARING and W. S. BROWER, in "Phase Diagrams for Ceramists 1975 Supplement", edited by E. M. Levin, C. R. Robbins, H. F. McMurdie and M. K. Reser (The American Ceramic Society, Columbus, OH, USA, 1975) Fig. 4340, p. 118.
14. J. J. LANDER, in "Phase diagrams for Ceramists", edited by E. M. Levin, C. R. Robbins, H. F. McMurdie and M. K. Reser (The American Ceramic Society, OH, 1964) Fig. 205, p. 96.
15. H. V. WARTENBERG and E. PROPHET, *ibid.*, Fig. 258, p 110.
16. R. S. ROTH, J. L. WARING and W. S. BROWER, in "Phase diagrams for Ceramists 1975 Supplement", edited by E. M. Levin, C. R. Robbins, H. F. McMurdie and M. K. Reser (The American Ceramic Society, Columbus, OH, USA, 1975) Fig. 4347, p. 121.
17. M. TAKATA and K. KAGEYAMA, *J. Am. Ceram. Soc.* **72** (1989) 1955.
18. K. WAKINO, K. MINAI and H. TAMURA, *ibid.* **67** (1984) 278.

Received 25 March
and accepted 20 August 1993